Supplementary Information

Distinguishing Metastatic Triple Negative Breast Cancer from Non-metastatic Breast Cancer using SHG Imaging and Resonance Raman Spectroscopy

Ethan Bendau[2+], Jason Smith[3+], Lin Zhang[4], Ellen Ackerstaff[5], Natalia Kruchevsky[5], Binlin Wu[6], Jason A. Koutcher[5, 7, 8, 9], Robert Alfano[4], and Lingyan Shi[1*]

[1.] Department of Bioengineering, University of California, San Diego, La Jolla, CA 92093

[2.] Department of Biomedical Engineering, Columbia University, New York, NY 10027

[3.] Department of Biomedical Engineering, Rensselaer Polytechnic Institute, Troy, NY 12180

[4.] Institute for Ultrafast Spectroscopy and Lasers, The City College of New York, New York, NY 10031

[5] Department of Medical Physics, Memorial Sloan Kettering Cancer Center, New York, NY 10065

[6.] Physics Department and CSCU Center for Nanotechnology, Southern Connecticut State University, New Haven, CT 06515

[7.] Department of Medicine, Memorial Sloan Kettering Cancer Center, New York, NY 10065

[8.] Molecular Pharmacology and Chemistry Program, Memorial Sloan Kettering Cancer Center, New York, NY 10065

[9.] Weill Cornell Medical College, Cornell University, New York, NY 10065

+ These authors contributed equally

* For correspondence: Lingyanshi@ucsd.edu

Supplementary Figures:

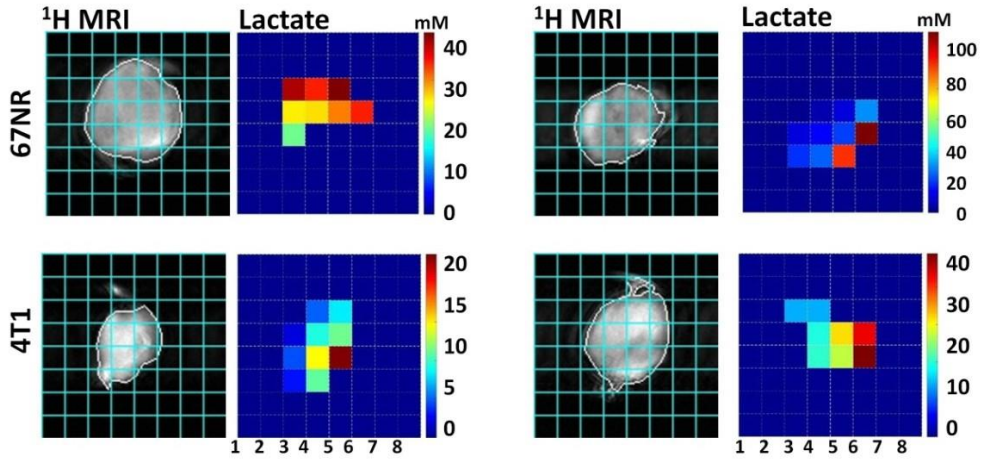

Figure S1: Lactate concentration maps of additional two 67NR (top row) and 4T1 tumors (bottom row) with corresponding anatomical MR images of the lactate MR slice, demonstrating the spatial lactate heterogeneity across different tumors. Areas that appear to be more necrotic on the T_2-weighted reference images (bright spots) display the lowest or no lactate. A grid (cyan) representing the in-plane lactate pixels, each 2 mm x 2 mm, is overlaid on the reference anatomical tumor MR images. The slice thickness for each tumor respectively are: 7 mm (top left), 6 mm, (top right), 4.5 mm (bottom left), and 5 mm (bottom right), resulting in corresponding pixel sizes for the lactate maps of 28 mm^3, 24 mm^3, 18 mm^3, and 20 mm^3. Of note is that edge pixels, such as 6,4 (top right), may overestimate the lactate concentration, due to exclusion of the skin layer from the tumor mask used to calculate the lactate concentration (thus, reducing tissue volume in the pixel) and potential 'bleed through' of the lactate signal from a neighboring pixel because of the point spread function, partially exacerbated by the spatially applied Hamming filter and a small pixel fraction of tumor tissue.

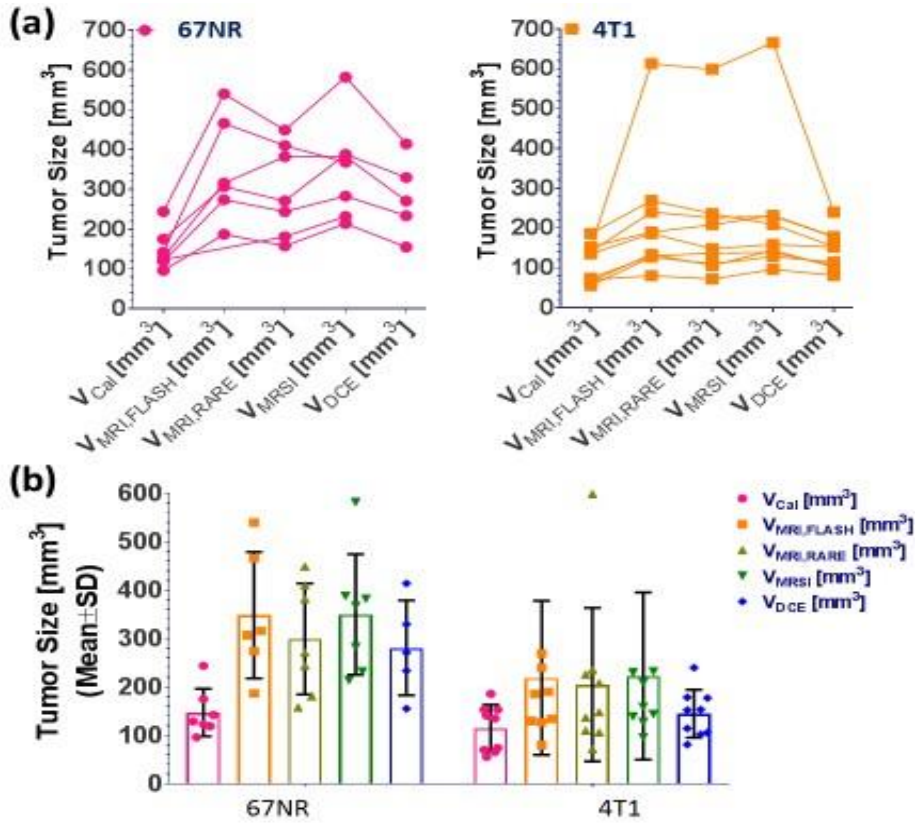

Figure S2: Comparison of tumor volumes determined by sliding jaw caliper and various MRI methods for each tumor type: (a) Tumor volume by different measures for each tumor and **(b)** averaged for each tumor type with each symbol representing single tumor measurements (n = 5-7 for 67NR and n = 9 for 4T1 tumors). Abbreviations: V_{Cal}, tumor volume by sliding jaw caliper; $V_{MRI,FLASH}$ and $V_{MRI,RARE}$, multi-slice ^{1}H MRI acquired with two different pulse sequences (FLASH and TurboRARE) and 1 mm thick slices; V_{MRSI}, single slice ^{1}H MRI with the same slice thickness as the slice for the lactate acquisition; V_{DCE}, multi-slice ^{1}H MRI acquired with the FLASH pulse sequence, 1 mm slice thickness and 4-7 slices dependent on tumor size (tumor volume covered by the DCE-MRI acquisition). Besides one 4T1 tumor, V_{DCE} typically covered the entire tumor, as can be seen from the similarity between all MR-based tumor volumes for each tumor. The tumor volumes determined by MR methods were consistently higher than V_{Cal}.

($V_{MRI,RARE}$ and V_{MRSI} *versus* VCal, respectively: $P < 0.05$, 2-way ANOVA with Sidak multiple comparison test and swapped direction).

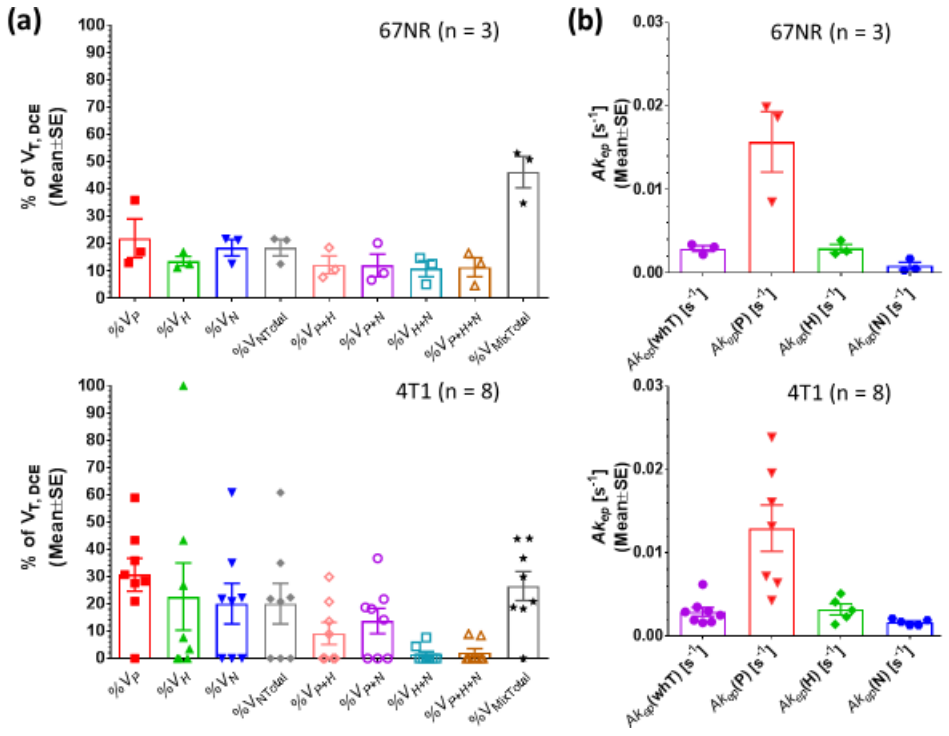

Figure S3: Tumor vascularity-based microenvironmental characteristics for 67NR (n = 3) and 4T1 (n = 8) tumors grown in the mammary fat pad of BALB/c mice. (a) Volume fractions V of tumor volume assessed by DCE-MRI and associated with tumor areas that are well vascularized (well-perfused, subscript P), less perfused (hypoxic, subscript H), leaking contrast agent into tissue (necrotic, subscript N), and mixtures thereof (indicated by the combined subscripts $_{P+H}$, $_{P+N}$, and $_{P+H+N}$). V_{NTotal} is the sum of $\%V_N$ and the volume fraction of the tumor with no contrast agent uptake, while $V_{MixTotal}$ is the sum of all tumor areas characterized by more than one environmental characteristic. Notably, none of the 67NR tumors and only 2/8 4T1 tumors had tumor areas without any contrast agent uptake, with those areas representing only 0.12% and 0.012% of these 2 tumors respectively. (**b**) Vascular blood flow and permeability (Ak_{ep}), a marker for tumor perfusion, for the whole tumor (whT) and the respective tumor fractions that are well perfused (P), have reduced perfusion (H), or little to no vascular perfusion (N). The 2-

tailed, paired t-Test showed that $Ak_{ep}(P) > Ak_{ep}(H)$ ($P < 0.1$, n=4), $Ak_{ep}(P) > Ak_{ep}(N)$ ($P < 0.05$, n=5), and $Ak_{ep}(H) > Ak_{ep}(N)$ ($P < 0.05$, n=2), for the 4T1 tumors with the respective vascular feature; for 67NR, $Ak_{ep}(P) > Ak_{ep}(H)$ ($P < 0.1$, n=3), $Ak_{ep}(P) > Ak_{ep}(N)$ ($P<0.1$, n=3), and $Ak_{ep}(H) > Ak_{ep}(N)$ ($P < 0.01$, n=3) . The vascular blood flow and permeability for the whole tumor, or the well-perfused and hypoxic tumor areas did not differ significantly between 67NR and 4T1 tumors ($P > 0.5$, unpaired, two-tailed t-Test), while $Ak_{ep}(N)$ tended to be lower in 67NR than in 4T1 ($P = 0.0748$, unpaired, two-tailed t-Test).

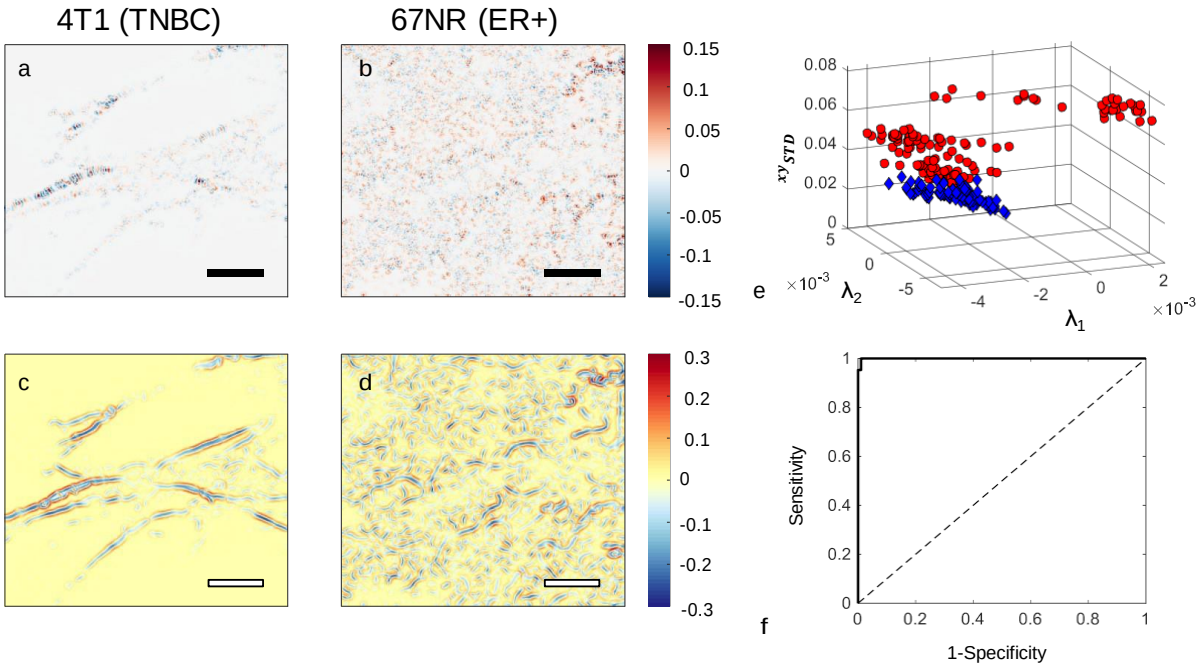

Figure S4: Two representative eigenvalue (λ_1 and λ_2) maps obtained via the 2D Hessian for 4T1 (a,b) and 67NR (c,d). The average of all non-zero λ values per image, along with the standard deviation of the Hessian cross-term, is plotted for illustration (e). Carrying out a LOOCV through SVM with these three features resulted in sensitivity, specificity and accuracy of 97.9%, 97.8% and 97.7% respectively (AUC = .9981).

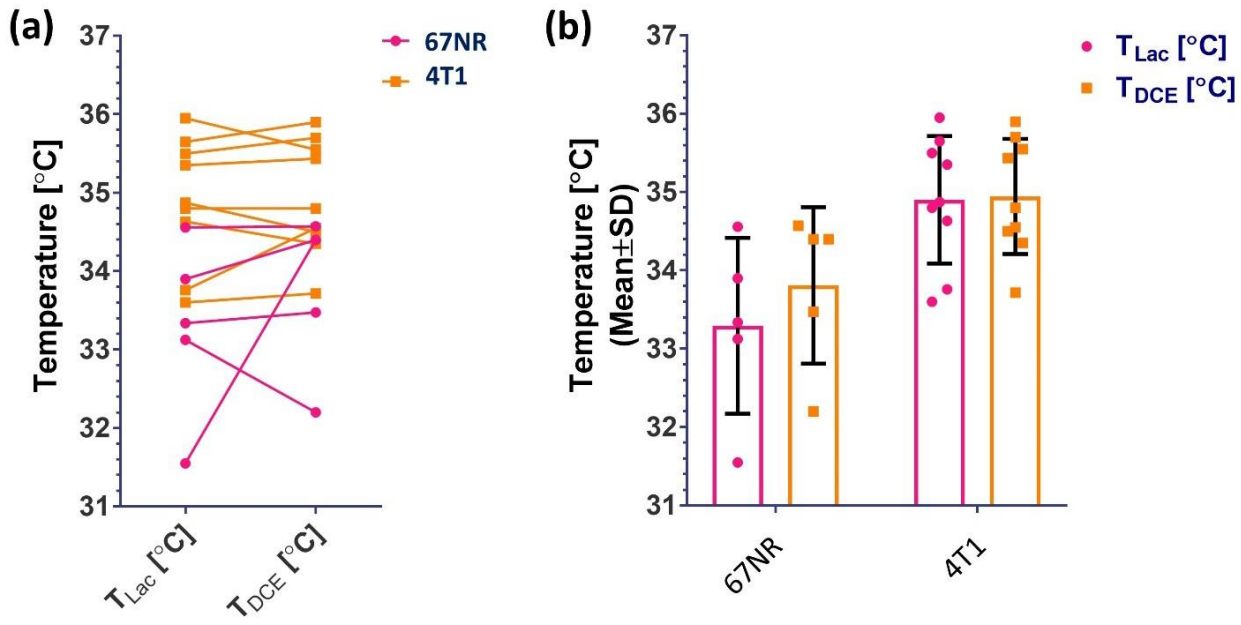

Figure S5: For each tumor type, animal core temperatures are comparable for the lactate (T_{lac}) and DCE-MRI (T_{DCE}) scans respectively (2-way ANOVA with Sidak multiple comparison), shown for corresponding scans in **(a)** and averaged in **(b)**. The difference of the averaged animal temperatures between tumor types for the lactate and DCE-MRI scans are 1.6 ^{0}C and 1.1 ^{0}C, respectively. Assuming a 1% false discovery rate, there is no difference between the mouse body temperatures for the 2 tumor types (unpaired t-Test, not assuming consistent standard deviation (SD), 2-state step-up method of Benjamini, Krieger and Yekutieli).